meteorology

MDPI

Article

Meteorological Drivers of Solar Resource Variability and Solar Energy Applications: Evidence from Eight Sites in Zambia

Harrison Likashi [1], Rekha Rajan [1,*], Orleans Mfune [2] and Reccab O. Manyala [1]

[1] Department of Pure and Applied Physics, University of Zambia (UNZA), Lusaka 10101, Zambia; likashiharrison@gmail.com (H.L.); reccab.manyala@unza.ac.zm (R.O.M.)
[2] Department of Geographical Sciences, Environmental and Planning, University of Zambia (UNZA), Lusaka 10101, Zambia; orleans.mfune@unza.ac.zm
* Correspondence: rrajan@unza.ac.zm

Abstract

Solar photovoltaic system (PV) design in some tropical regions often applies generalised monthly resource assumptions, yet seasonal solar resource deficits and their meteorological drivers vary significantly across locations. This study examined spatial and seasonal variability in solar irradiance across eight sites in Zambia, identified its meteorological relations, and assessed implications for photovoltaic battery bank autonomy. Ten years of ground solar resource observations from the Southern African Science Service Centre for Climate Change and Adaptive Land Management (SASCAL) were analysed alongside NASA POWER satellite data and Meteonorm sunshine duration estimates. Temporal, spatial, worst-month, and correlation analyses were conducted, and irradiance conditions were translated into battery bank autonomy requirements using the Southampton Solar Autonomy Calculation Tool. Depending on location, results showed a consistent annual irradiance cycle, peaking in September–October and declining during either the rainy or cool dry season. Kalabo and Samfya showed relatively high and stable irradiance, while Mpulungu and Mwinilunga recorded lower values and deeper seasonal minima. Worst-month analysis identified January as critical for northern and lake-neighbouring sites, and June–July for plateau, western, and southern sites. Cloud amount, precipitation, and relative humidity were the most consistent negative drivers, while temperature showed positive associations and wind effects varied by site. Sunshine duration explained spatial contrasts more effectively than minor differences in astronomical day length. These findings demonstrate that a uniform national "worst-month" criterion may misrepresent local seasonal energy risks and photovoltaic battery bank autonomy requirements. Site-specific solar resource and meteorological assessment should therefore guide PV and storage system design in Zambia and comparable tropical regions.

Keywords: solar resource variability; meteorological drivers; solar irradiance; worst-month analysis; sunshine duration; photovoltaic energy

Check for updates

Academic Editors: Paul Williams and Jimy Dudhia

Received: 7 August 2026
Revised: 5 October 2026
Accepted: 12 October 2026
Published: 20 November 2026

Copyright: © 2026 by the authors. Licensee MDPI, Basel, Switzerland. This article is an open access article distributed under the terms and conditions of the Creative Commons Attribution (CC BY) license.

1. Introduction

Solar energy has become central to global efforts to expand electricity access, enhance energy security, and reduce dependence on fossil-based energy generation, especially in regions with strong photovoltaic (PV) potential and persistent energy shortfalls [1–3]. In Zambia, this transition is critical and urgent because the national electricity system is heavily dependent on hydropower which is increasingly becoming vulnerable to climate-induced

shocks. As a result, the country has, over the past six years, experienced recurring load-shedding which has intensified interest in PV systems for a more diversified and resilient generation mix [4,5]. Similarly, several studies on African energy systems have stressed the need for integration of climate-resilient energy systems when planning for reliable PV power supply systems [6,7].

While there is clearly a global trend towards solar energy technology development and deployment, scientific work is still grappling with understanding factors that affect the variability of solar irradiance at different locations. The viability of solar energy for practical applications does not only depend on the magnitude of the resource but also on its temporal and spatial variability [8,9]. Solar irradiance reaching the surface is controlled by atmospheric conditions, such as clouds, aerosols, humidity, and precipitation [10]. These all affect both the quantity and the spectral quality of radiation available for PV conversion. Cloud-related processes represent the largest source of uncertainty in irradiance characterisation [11]. In addition, broader reviews on PV performance consistently identify irradiance level, ambient temperature, humidity, and atmospheric transmissivity as key drivers of actual system output [7,12]).

Recent review studies further advance the case for evaluating meteorological drivers when investigating solar irradiance variability and its implications for solar PV energy applications. As shown in [13], PV output is shaped by interacting environmental controls rather than by irradiance alone, with cloud cover, ambient temperature, humidity, wind, aerosols, and soiling influencing both solar resource availability and conversion efficiency. Similarly, ref. [14] reports that irradiance, temperature, humidity, and dust-related effects are key determinants of PV performance, noting that humid conditions may increase dust adhesion on module surfaces and thereby intensify output losses. Taken together, these studies indicate that site-specific meteorological conditions are central both to explaining solar irradiance variability and to assessing how that variability translates into PV energy performance across different environments [13,14].

For solar energy planning, solar irradiance variability is a key design issue because it governs the sizing of both generation capacity and storage systems [8,15]. Comparative studies of irradiance datasets have shown that reliable site-specific solar resource assessment requires local validation [16]. This is because the performance of satellite-derived, reanalysis, and interpolated datasets varies with terrain, station density, and latitude. Similar work on renewable variability in Africa shows that meteorologically driven fluctuations in solar generation have direct implications for the planning of reliable energy systems in regions that need to diversify a climate-sensitive electricity supply [3,6].

This challenge is especially relevant in Zambia. Although the country is widely recognised as having favourable solar potential, with annual global horizontal irradiation ranging from approximately 1900 to 2100 kWh/m^2 across much of the country [3], strong mean availability does not suggest uniformity in conditions across the annual cycle or across locations. In [5], pronounced spatial differences in global irradiance were predicted among major Zambian cities, and the World Bank's Zambia Solar Resource Atlas shows similar results at multiple reference stations [3]. In spite of these results, the existing literature on Zambia focuses more on PV feasibility, techno-economic performance, and deployment potential [1,4]. This literature is lacking in empirical, multi-site assessment of solar irradiance variability and its meteorological associations based on long-term ground observations across Zambia's contrasting climatic environments.

In the context of solar energy planning, worst-month analysis is widely recognised as a valuable tool because it identifies the seasonal period during which solar availability is most constrained, thereby serving as the reference condition for cautious and realistic PV and storage system design [8,17]. Guidelines on solar resource assessment consistently

emphasise that seasonal characterisation is important for effective planning in environments where weather variability may affect monthly generation performance [8,9].

However, empirical evidence for Zambia remains scarce outside Lusaka (UNZA), with limited studies addressing the timing and magnitude of worst-month conditions across different climatic environments. Researchers have not yet simultaneously analysed multiple meteorological parameters across diverse zones, leaving a gap in our understanding of how irradiance variability is driven by local atmospheric processes. Comparative studies in tropical regions, such as in [18], demonstrate that the Intertropical Convergence Zone (ITCZ) exerts a strong influence on seasonal irradiance variability, underscoring the need for site-specific analysis in Zambia's heterogeneous climate.

Furthermore, while satellite products such as CERES and HelioClim provide valuable regional coverage, uncertainty with regard to their effectiveness under cloudy tropical conditions has been documented [9]. As yet, no studies have systematically compared ground-based and satellite data in Zambia to assess reliability across different meteorological regimes. Addressing this methodological gap is essential for justifying combined approaches that integrate station observations with satellite datasets, particularly in regions where cloud cover and humidity strongly affect irradiance retrieval accuracy.

Against this background, this study investigates the meteorological drivers of solar resource variability in Zambia using a ten-year monthly dataset from eight sites representing the country's diverse geographical and environmental conditions. The study addresses three questions: (1) How does solar irradiance vary temporally and spatially across the selected sites? (2) Which meteorological variables are most strongly associated with that variability? (3) Which months represent the most critical seasonal constraints for solar energy applications at each site? The study advances the existing literature by providing a distinct, multi-site, observationally grounded assessment of Zambia's solar resource that links irradiance behaviour to locally relevant meteorological drivers and identifies site-specific worst-month conditions for determining DoA for PV battery bank sizing, thereby supporting more climate-responsive PV planning in Zambia and other climatically diverse regions in sub-Saharan Africa.

2. Materials and Methods

2.1. Study Area

The study was carried out at eight sites distributed across varying climatic regimes in Zambia, including Kitwe, Kalabo, Mpulungu, Mwinilunga, Namwala, Samfya, Serenje, and UNZA (Lusaka), as shown in the map in Figure 1.

The sites were purposively selected to represent Zambia's broad environmental diversity, including northern and lake-influenced areas, the central plateau, and the relatively drier western and southern regions. This diversity in environmental conditions is important because its influence on solar resource availability can be significant [19].

Table 1 shows the agro-ecological region, latitude, longitude, and altitude of the study sites.

The altitudes of the eight sites range from 801 m (Mpulungu) to 1395 m (Serenje). While this study focuses on meteorological drivers of irradiance variability, differences in elevation and local terrain may also contribute to spatial contrasts in solar resource availability.

Zambia's climate gradient ranges from humid tropical conditions in the north, characterised by annual rainfall exceeding 1200 mm, to drier savanna conditions in the south with as little as 600 mm of rain per year, with attendant differences in cloud cover, humidity, and solar availability across agro-ecological regions [3,5]. The geographical distribution of the eight sites was intended to capture these climatic contrasts and provide a basis for assessing how regional conditions are associated with solar resource variability.

Table 1. Characteristics of the selected study sites in Zambia.

Station Name	AER	Latitude	Longitude	Altitude (m)
CBU-Kitwe	III	−12.81	28.24	1220
Kalabo	IIB	−14.99	22.68	1018
Mpulungu	III	−8.77	31.12	801
Mwinilunga	III	−11.74	24.43	1360
Namwala	IIA	−15.32	26.43	998
Samfya	III	−11.37	29.56	1194
Serenje	III	−13.23	30.22	1395
UNZA-Lusaka	IIA	−15.39	28.33	1260

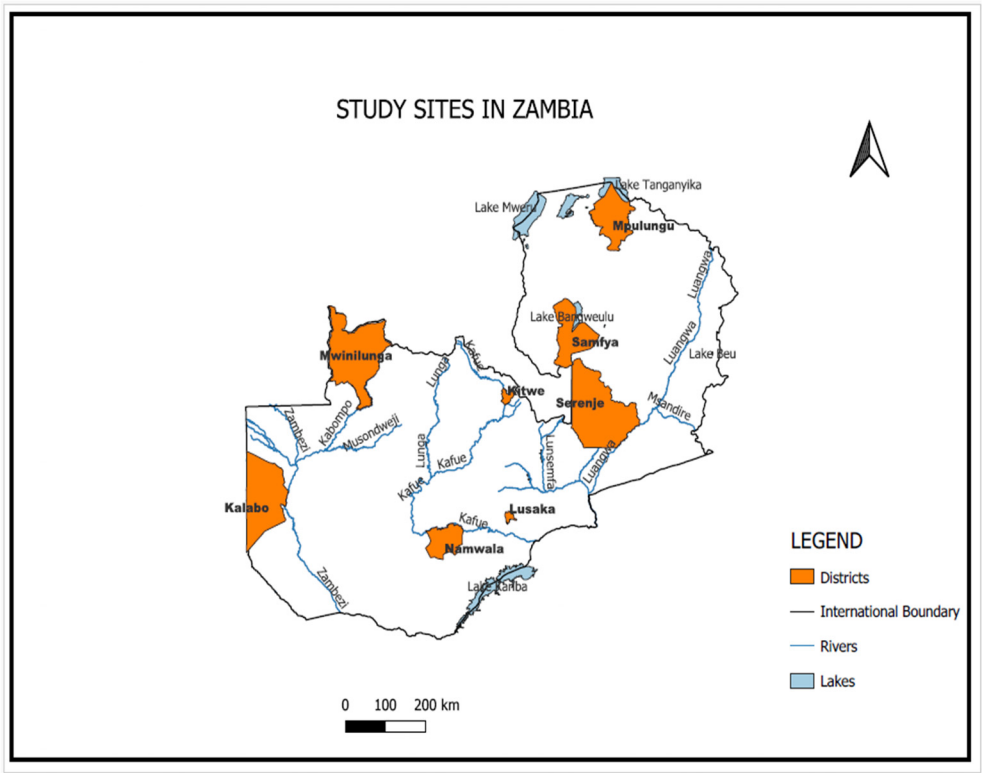


Figure 1. Geographical spread of the eight study sites.

2.2. Data Sources

The core dataset consisted of daily and monthly average global solar irradiance and associated meteorological records obtained from the SASSCAL automated weather station network in Zambia. This data was accessed through the University of Zambia's Department of Geographical Sciences, Environmental and Planning. SASSCAL stations are equipped with calibrated pyranometers and automated data loggers that record solar irradiance and related meteorological parameters continuously, with data transmitted through remote terminal units (RTUs) to centralised repositories [20]. Because the instruments operate on fully automated logging systems, data were received in their original recorded form without manual field transcription. The main variables used from SASSCAL were global solar irradiance, air temperature, relative humidity, wind speed, and precipitation. Site-specific records fell within the broader monitoring period of 2014–2024. However, temporal coverage varied considerably across locations.

Complementary monthly data were sourced from NASA's Prediction of Worldwide Energy Resources (POWER) database, ref. [21], which includes data of all-sky surface shortwave irradiance, air temperature, cloud amount, precipitation, and relative humidity. While satellite products such as CERES and HelioClim provide valuable regional coverage, uncertainty about their effectiveness under cloudy tropical conditions has been documented. Owing to the absence of cloud amount measurements from SASSCAL ground stations, the variable was sourced exclusively from NASA POWER. Sunshine duration estimates were obtained from Meteonorm software. This software is a widely used climatological tool that interpolates measured data to generate estimates of surface radiation and sunshine hours, among other data [22]. In the present study, this software was used to provide contextual characterisation of seasonal atmospheric transparency at selected sites, using sunshine duration.

2.3. Instruments/Tools

In this study, three complementary instruments were used: Meteonorm, for modelling sunshine duration across the study sites; the Southampton Solar Autonomy Calculation Tool (PV01.Autonomy_Tool.01), for determining the number of days of autonomy (DoA) for PV battery bank sizing; and Python 3.14.6 for data processing and analysis. The Meteonorm software, version 8.2.0 was set as shown in Table 2.

Table 2. Settings of the Meteonorm software for modelling sunshine duration.

Item	Setting Used
Software	Meteonorm, version 8.2.0
Site definition	User-defined locations under the weather station module
Dataset	Meteonorm climate data
Global radiation setting	Corrected global radiation
Atmospheric turbidity	Interpolated
Calculation setting	Contemporary
Future scenario	RCP 2.6
Output format	Meteonorm

The Solar Autonomy Calculation Tool was applied to estimate PV battery storage requirements under different array-oversize factors. The tool applies a daily energy balance model using worst-month solar radiation and an array-oversize factor (CA). A CA value of 1.0 represents an array sized to meet the load under average worst-month conditions without additional loss allowance, while values of 1.1–1.25 allow for approximately 10–20% losses, improving reliability by reducing the required DoA.

Collectively, the tools provided a comprehensive framework for linking meteorological drivers to solar resource behaviour and for applying solar irradiance variability into practical PV battery bank designs in Zambia.

2.4. Data Handling

Because SASSCAL stations operate with automated logging and transmission, data were delivered in machine-recorded format and did not require transformation from manual records. Therefore, data handling was restricted to physical plausibility checks and consistency verification prior to analysis. These checks involved screening for values outside physically reasonable irradiance bounds, inspecting for timestamp inconsistencies, and

identifying flagged observations noted in the original SASSCAL quality reports. Monthly records were subsequently organised into a unified format across sites, variable labels and units were standardised, and series were verified for completeness prior to analysis. This degree of preprocessing was appropriate for the objectives of the present study because the analysis relied on monthly aggregates derived from automated observations and did not require high-frequency gap filling or imputation.

Prior to quality control, missingness ranged from 0.00% at Serenje to 9.71% at UNZA, with intermediate values of 0.14% at Namwala, 0.42% at CBU, 0.50% at Kalabo, 1.98% at Mpulungu, 5.85% at Samfya, and 7.75% at Mwinilunga. After cleaning, the daily irradiance record comprised 1433 observations at Namwala, 1591 at Serenje, 2075 at Samfya, 2133 at Mwinilunga, 3557 at Mpulungu, 3574 at CBU, 3652 at UNZA, and 4140 at Kalabo. Short gaps of up to three days were interpolated, whereas longer gaps were retained to preserve data integrity.

Data availability varied among sites because of differences in commissioning dates, operational continuity, and record completeness. To minimise bias arising from unequal record coverage, direct inter-site comparisons were restricted to periods of concurrent valid observations, while site-specific temporal, correlation, worst-month, and DoA analyses were conducted using the full quality-controlled dataset available for each station. The 2016–2017 period was the only interval with complete concurrent observations for all eight sites. Therefore, it was selected for figures requiring comparison across the full network for this study. For periods outside 2016–2017, comparisons involved only the subset of stations with concurrent valid datasets. Temporal characterisation, worst-month analysis, and meteorological correlation analysis were conducted using the full quality-controlled data record available for each site.

For the satellite-derived NASA POWER data, no further cleaning was undertaken. For the daily average global solar irradiance dataset obtained from SASSCAL, a screening range of 0–405 W/m^2 was applied in the Degree of Agreement (DoA) calculation. A lower limit of 0 W/m^2 was chosen because negative irradiance values are physically implausible, while the upper limit of 405 W/m^2 was adopted as a high-end plausibility threshold. This range corresponds closely with reported daily global solar exposure values of approximately 35 MJ/m^2/day, which represent the highest levels typically observed under clear-sky conditions worldwide [23]. For monthly averages, verification was limited to confirming that the extracted NASA POWER values corresponded to the specific site coordinates and time periods under analysis.

2.5. Analytical Methods

Temporal characterisation, worst-month analysis, and meteorological correlation analysis were conducted using the full quality-controlled record available for each site. Long-term monthly climate records were derived by aggregating all available observations for each calendar month across the study period. The worst month was defined as the calendar month with the minimum long-term mean irradiance among the resulting twelve-monthly climatological values, following the worst-month approach of [17]. This definition captures the recurrent climatological period of minimum solar resource availability at each site, rather than an anomalous minimum observed in a single year, thereby providing a robust reference for comparative assessment and system design. Spatial variability was further quantified using the long-term mean, the standard deviation, and the coefficient of variation of irradiance, enabling evaluation of both absolute and relative differences across sites.

The potential influence of astronomical day length on solar irradiance was assessed by comparing the calculated maximum day-length differences across the eight study sites with the magnitude of the observed irradiance variations. Because the inter-site range in

astronomical day length was found to be negligible (approximately 25.8 min), sunshine duration, which more accurately reflects the actual beam radiation fraction under prevailing local atmospheric conditions was adopted as the more informative contextual variable.

To characterise the observational stability of the identified worst-month condition, a non-parametric month-stratified bootstrap procedure with 100,000 resamples was applied. For each site, observations were resampled with replacement within each calendar month, after which monthly mean irradiance values were recalculated and ranked. Percentile-based 95% confidence intervals were obtained for the identified worst-month mean, and ranking stability was expressed as the proportion of bootstrap resamples in which the identified month retained the lowest rank. These statistics were used to interpret the stability of the observed worst-month classification, and were not used as inputs to the deterministic autonomy calculations.

Meteorological controls on global solar irradiance were assessed through Pearson correlation analysis. The analysis examined the relationships between monthly global solar irradiance and five key covariates: air temperature, relative humidity, precipitation, wind speed, and cloud amount. Correlation coefficients were calculated for each variable–irradiance pair at each of the eight study sites. Pearson correlation was selected because the objective was to describe bivariate relationships rather than to estimate independent causal effects of interrelated meteorological variables or to develop a predictive model. This approach, applied to the full available monthly time series, enabled the identification of both site-specific relationships and broader cross-site patterns of associations. Long-term daily average global irradiances and worst-month averages of global solar irradiances were used calculate DoA using the Solar Autonomy Calculation Tool. The results from DoA contextualised the bivariate analysis by translating statistical associations into practical PV applications.

3. Results and Discussion

3.1. Comparison of Satellite-Derived Solar Irradiance Against Ground Measurements

Figure 2 compares monthly ground-based global solar irradiance measurements recorded at the University of Zambia, Lusaka, with corresponding NASA POWER satellite-derived estimates.

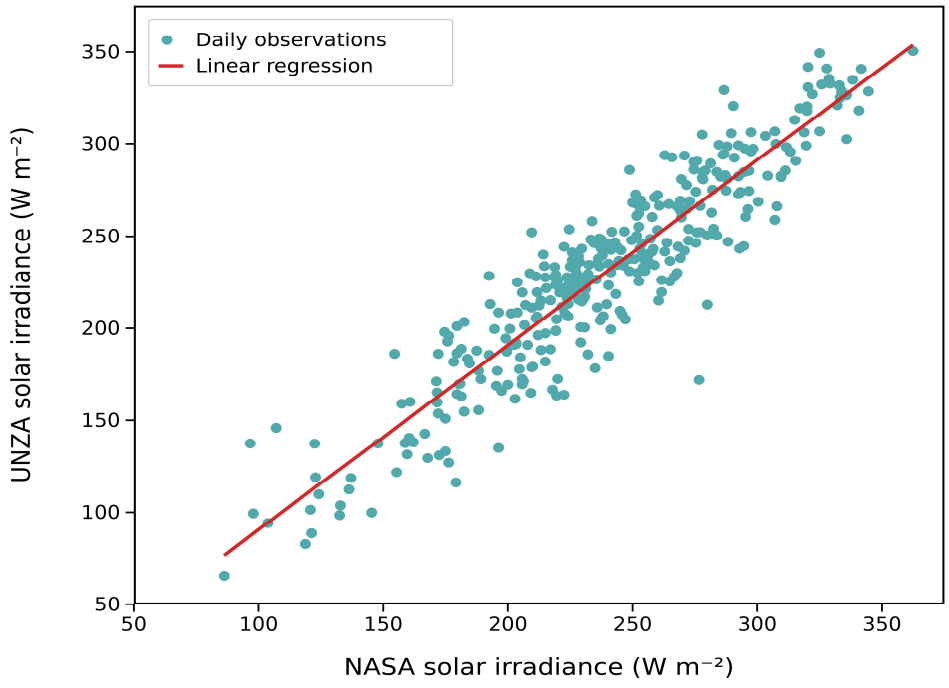


Figure 2. Ground vs. satellite agreement in solar irradiance.

The regression analysis in Figure 2 shows strong agreement ($R = 0.926$, $R^2 = 0.857$), suggesting that the NASA satellite dataset reproduced the principal seasonal and inter-monthly variability observed on the ground. A negative mean bias deviation (-9.045 W m^{-2}) indicates modest systematic underestimation relative to ground measurements, while the mean absolute deviation (17.145 W m^{-2}) and root mean square deviation (22.412 W m^{-2}) suggest moderate discrepancies, including occasional larger departures. NASA POWER therefore provides a useful complementary source of solar resource information for Zambia, although locally calibrated ground observations remain important for site-specific PV-yield assessment and system sizing.

3.2. Temporal Variability of Solar Irradiance

Monthly irradiance across the eight sites exhibited a recurring annual cycle. Values generally increased toward the end of the rainy season, reached maximum levels during September–October, and declined during either the early rainy season or the cool–dry season, depending on location. Figure 3 shows the monthly irradiance profiles for the 2016–2017 period, the only interval with complete concurrent observations across all eight sites.

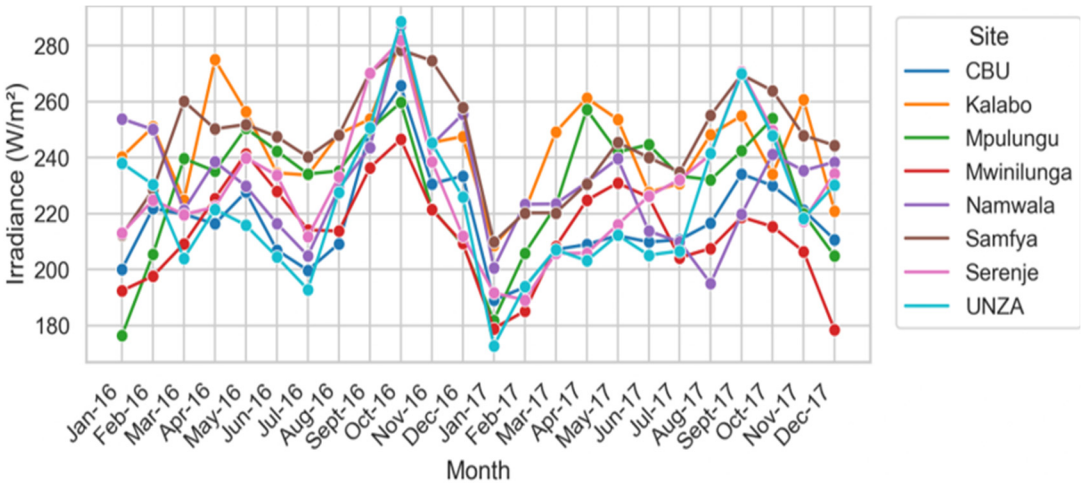


Figure 3. Monthly global solar irradiance patterns across the eight study sites for the 2016–2017 comparison period.

The pattern shown in Figure 3, remained consistent across all the comparison periods (2014, 2015, 2016–2017, 2018, 2019, 2020, and 2021–2024). This demonstrates that the seasonal structure is governed by persistent atmospheric drivers rather than short-term year-to-year variability. The regularity of this cycle aligns with the prevailing Inter-Tropical Convergence Zone (ITCZ) which governs Zambia's rainfall and cloud cover regime [3,5]. It is also consistent with broader findings on solar generation seasonality in southern Africa [6].

The September–October irradiance maximum corresponds to a period of dry, clear atmospheric conditions preceding the onset of the rainy season, during which atmospheric water vapour and cloud fraction are at seasonal minima [5,7]. In contrast, the wet season decline reflects an inverse pattern, with increased cloudiness, moisture loading, and precipitation associated with ITCZ, which progressively reduces surface irradiance from approximately November onward [3,6]). Although the amplitude of the seasonal minima varied somewhat across years, the timing of both peaks and troughs remained broadly stable, supporting the use of monthly long-term averages as a reliable basis for seasonal solar resource characterisation in Zambia [8,16].

3.3. Spatial Contrasts in Solar Resource

Clear spatial differences in mean irradiance were observed across the study sites. Kalabo and Samfya consistently recorded the highest mean irradiance, at 253.1 W/m^2 and 258.0 W/m^2 respectively, while Mpulungu and Mwinilunga recorded the lowest, at approximately 216–220 W/m^2. UNZA and Serenje occupied intermediate positions, and CBU and Namwala varied between intermediate and relatively higher irradiance levels depending on season. The spatial distribution of irradiance variability is further illustrated using the variability ranking presented in Figure 4.

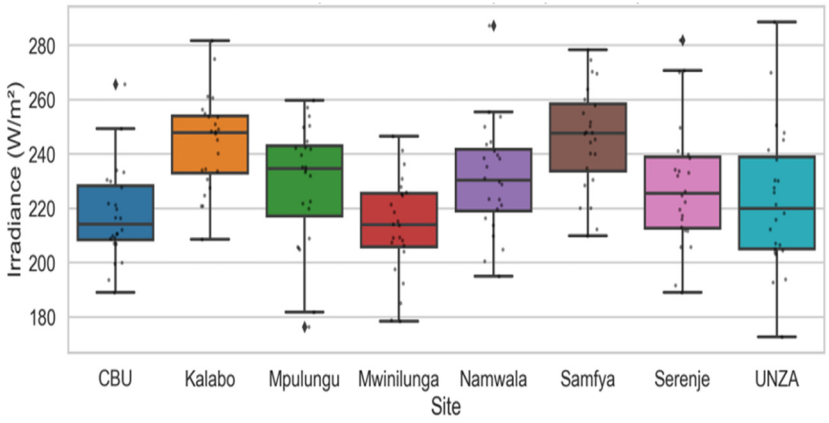


Figure 4. Boxplot comparison of monthly global solar irradiance across the eight study sites for the period 2016–2017.

Figure 4 shows observed differences in tail behaviour, whiskers, mean values and interquartile ranges for the 2016–2017 comparison period. Boxes represent the interquartile range (25th–75th percentiles), and horizontal lines within the boxes indicate the median. Whiskers extend to the most extreme observations within 1.5 times the interquartile range of the lower and upper quartiles. Black diamond-shaped markers beyond the whiskers indicate outlying observations, while the small overlaid dots represent individual observations. The results suggest that the spatial structure of Zambia's solar resource constitutes a resilient climatological feature rather than a period-specific irregularity, although local topography may modulate irradiance at finer scales. The finding is consistent with long-term patterns identified in the World Bank Solar Resource Atlas [3]. Figure 5 complements the boxplot comparison by summarising site-level mean irradiance, standard deviation, and coefficient of variation.

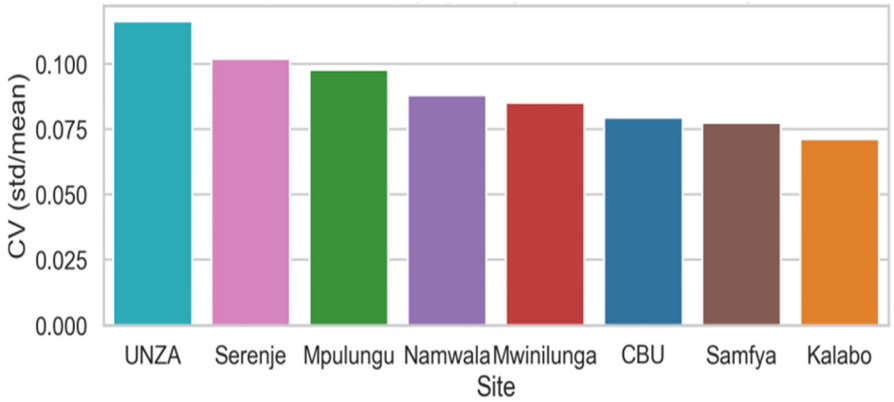


Figure 5. Spatial variability of monthly solar irradiance across the study sites based on summary dispersion measures.

These rankings in variability remained stable across all comparison periods, indicating a persistent spatial structure in Zambia's solar resource.

3.4. Worst-Month Conditions

The lowest observed monthly irradiance was site-specific, indicating that a single nationally prescribed design month does not represent the seasonal diversity of Zambia's solar resource. January was the month with lowest observed irradiance at Mpulungu, Mwinilunga, Samfya, Kitwe, and Serenje, whereas June had the lowest at Lusaka and Kalabo, and July the lowest at Namwala. These findings are similar to the low solar patterns predicted by both [5] and [3] for reference stations across Zambia. January emerged as the lowest solar resource month at Mpulungu, Mwinilunga, Samfya, CBU in Kitwe, and Serenje, whereas June was the lowest at UNZA (Lusaka) and Kalabo, and July at Namwala. This spatial differentiation reflects a systematic north–south contrast in the dominant seasonal drivers. In northern sites, ITCZ-related cloudiness and moisture loading are most pronounced, producing the strongest suppression of irradiance. By contrast, plateau, western, and southern sites reach their irradiance minimum during the June–July cool–dry period, when reduced solar elevation angles rather than cloud cover constitute the primary constraint on received solar radiation.

When viewed in terms of agro-ecological regions, Table 3 indicates a distinct regional stratification in worst-month solar resource conditions. The magnitude of the worst-month minima varied across sites as shown in Table 3 below.

Table 3. Worst-month solar irradiance by study site.

Site	Worst Month	Min Irradiance (W/m^2)	AER
Mpulungu	January	182	III
Mwinilunga	January	191.5	III
Samfya	January	197.4	III
Lusaka	June	202	IIA
Namwala	July	206.8	IIA
Kitwe	January	207.4	III
Serenje	January	213.8	III
Kalabo	June	230.3	IIB

To characterise the observational stability of the identified worst-month conditions, bootstrap 95% confidence intervals and rank-1 probabilities were calculated for each site (Table 4). The statistics describe the stability of the observed monthly classification and do not alter the deterministic autonomy calculations, which use the lowest observed long-term monthly mean at each site.

January showed high ranking stability at Mpulungu and Serenje, which retained the lowest rank in 99.4% and 90.6% of bootstrap resamples, respectively, while July at Namwala showed moderate stability (88.9%). The identified worst months at Kitwe, Kalabo, Samfya, Mwinilunga, and Lusaka had lower rank-1 probabilities, ranging from 48.9% to 78.2%, indicating that neighbouring months had comparable low-resource conditions. At these sites, the reported month represents the lowest observed monthly mean within a broader low-resource seasonal interval rather than as a distinctly isolated minimum.

Nevertheless, the bootstrap assessment supports the broader regional pattern. Agro-ecological Region III sites generally reached their lowest irradiance during the rainy season,

whereas Region II sites reached their minimum during the cool-dry season. Kalabo retained the highest worst-month irradiance among the study sites, and the approximately 48 W/m^2 difference between the highest and lowest worst-month irradiance values indicates meaningful spatial variation in conditions relevant to PV battery bank sizing. The deterministic autonomy calculations therefore use the lowest observed long-term monthly mean at each site, while the bootstrap results provide context for interpreting the stability of the corresponding low-resource condition.

Table 4. Bootstrap confidence and stability of worst-month identification.

Site	Worst Month	95% CI, (W/m^2)	Rank-1 Probability, %
Kitwe	January	189.6–227.1	78.2
Kalabo	June	224.3–235.8	60.4
Mpulungu	January	175.6–189.8	99.4
Mwinilunga	January	183.1–199.8	57.0
Namwala	July	203.8–209.9	88.9
Samfya	January	191.0–207.7	73.4
Serenje	January	205.2–226.5	90.6
Lusaka	June	194.2–207.9	48.9

3.5. Day Length, Sunshine Duration, and Atmospheric Transparency

Astronomical day length was calculated using:

$$dn = \frac{2}{15}\cos^{-1}(\tan\delta \tan\varphi)$$

where dn is daylength in days, φ latitude in degrees (positive north, negative south), and δ solar declination angle (in degrees).

The seasonal and spatial variation in daylight across the eight sites is shown in Figure 6 with the theoretical interval between sunrise and sunset dependent primarily on latitude and solar declination.

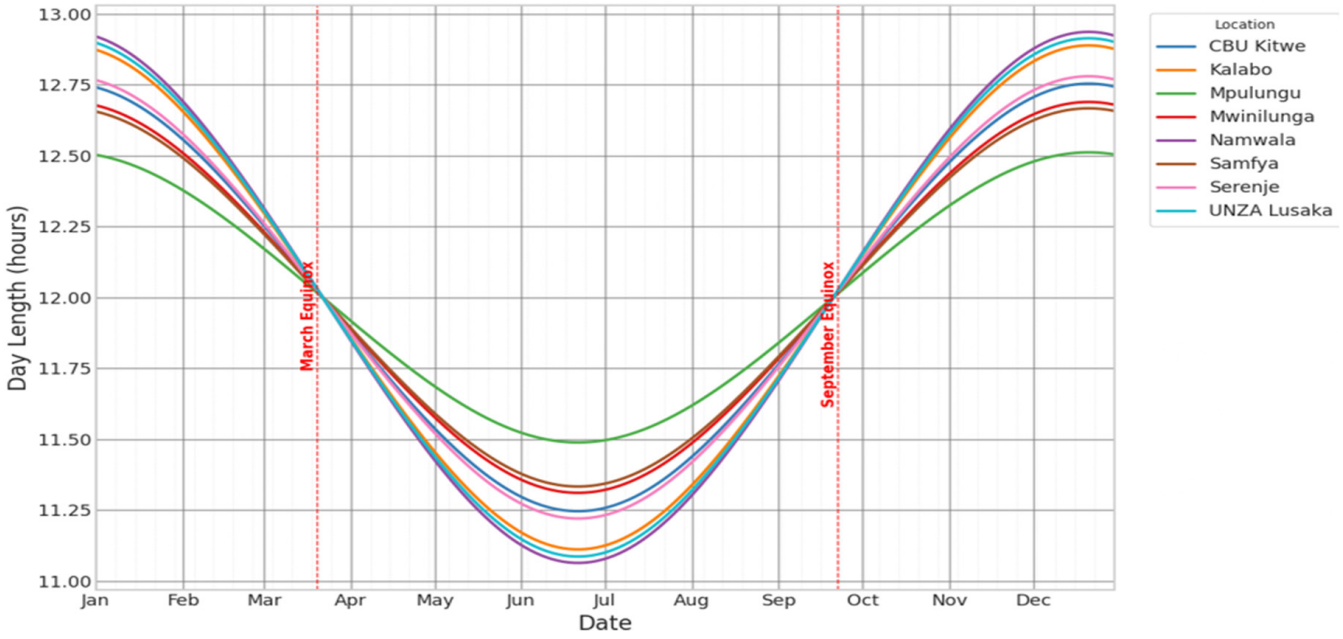


Figure 6. Astronomical day length across the eight study sites, showing minimal inter-site variation.

Figure 6 shows that day length does vary seasonally, and therefore contributes to seasonal differences in potential surface irradiance. Although solar elevation angle and altitude may influence the intensity of radiation received at the surface by affecting atmospheric path length and attenuation [24], the inter-site variation in astronomical day length across the eight study locations was very small, with a maximum difference of only about 25.8 min. This narrow range is insufficient to explain the pronounced spatial contrasts observed in solar irradiance variability across the eight sites.

As shown in Figure 7, sunshine duration varied much more strongly across seasons and sites than astronomical day length.

While [25] recognised a December maximum and June minimum in sunshine hours at the national scale, the present results show that this pattern reflects astronomical sunshine duration rather than the actual duration of bright sunshine received at the surface. By distinguishing realised sunshine duration from theoretical day length, the Meteonorm outputs further demonstrate that sunshine availability is not nationally uniform but varies markedly across sites and seasons in response atmospheric transparency. By contrast, the onset of the hot season in September and October, despite coinciding with high global surface irradiance, is accompanied by a decline in sunshine duration, indicating that atmospheric transparency begins to deteriorate before the full onset of the rainy season. The present results from Meteonorm therefore help explain why locations with broadly similar day-length conditions can still exhibit substantial differences in observed irradiance and PV energy potential.

3.6. Meteorological Drivers of Solar Irradiance Variability

Solar irradiance variability in Zambia shows a direct relationship with atmospheric moisture and cloud-related processes, which function as the primary drivers. The study sites experienced continuous decreases in solar irradiance because of cloud cover and relative humidity and precipitation, which served as the primary factors that reduced sunlight exposure. The findings confirm previous research into PV and solar energy systems which has demonstrated that atmospheric conditions, particularly cloud cover and humidity and aerosol levels and transmissivity changes, determine the amount of solar radiation that reaches the Earth surface, affecting photovoltaic energy production [7,13,14]. This study demonstrates that these drivers function as fundamental elements which establish direct links to the studied locations through their impact on controlling relationships between northern lake areas and areas in the drier western plateau territory.

The CBU ground data record for Kitwe shows an apparent post-2022 shift across several variables. In the absence of complete metadata on station maintenance, sensor calibration, logging configuration, and site exposure, this shift cannot be attributed conclusively to climatic variability. The observations were retained after plausibility checks but are interpreted with caution, and no climatic inference is drawn from this station-specific discontinuity.

(a) Cloud amount.

In this study, 'cloud amount' refers to the monthly mean fractional coverage of the entire visible sky by clouds (range 0–1), as provided by the NASA POWER dataset. Higher values indicate a larger proportion of the sky dome obscured by cloud, which reduces the transmission of direct and diffuse shortwave radiation to the surface. Figure 8 shows the variation in cloud amount across the eight study sites.

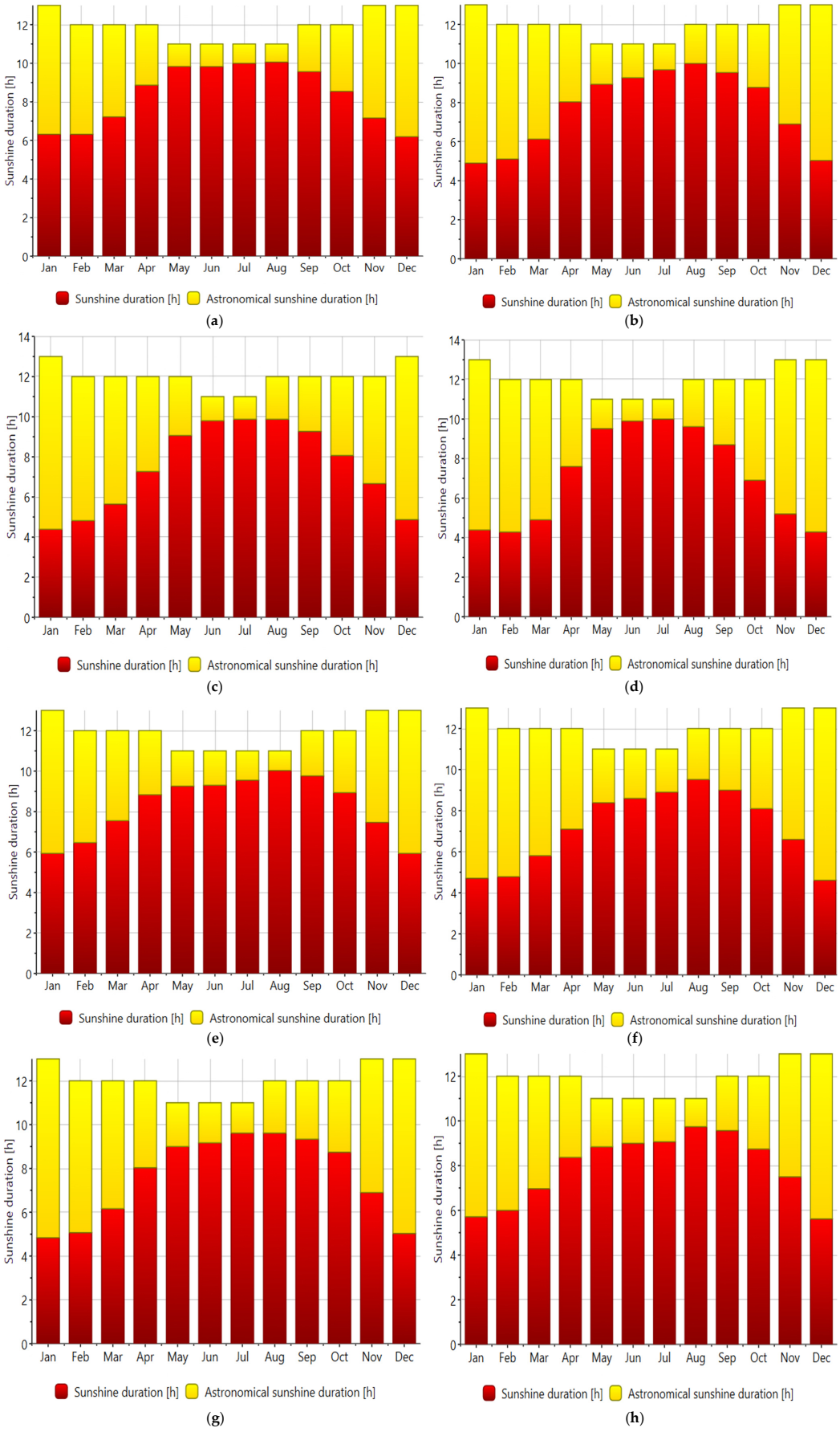


Figure 7. Seasonal sunshine-duration profiles for the eight study sites: (**a**) Kalabo, (**b**) CBU Kitwe, (**c**) Mwinilunga, (**d**) Mpulungu, (**e**) Namwala, (**f**) Samfya, (**g**) Serenje, and (**h**) UNZA (Lusaka).

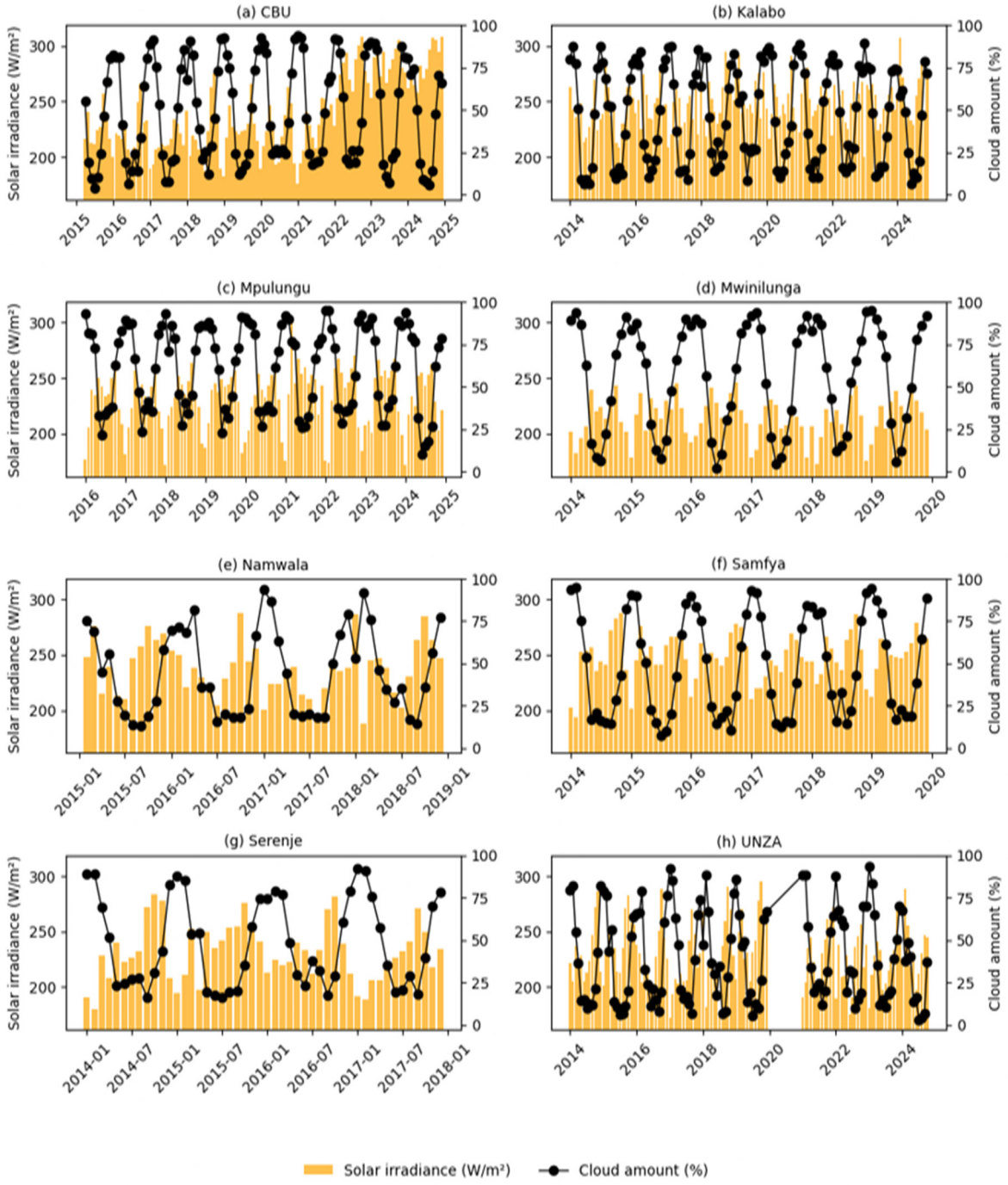


Figure 8. Relationship between cloud amount and global solar irradiance across the study sites.

As shown in Figure 8, cloud amount exhibited the strongest and most direct negative relation with solar irradiance across the eight study sites. This observation confirms that cloudiness is the dominant immediate control on shortwave attenuation in Zambia. This is as expected, because increased cloud cover reduces the transmission of direct solar radiation through reflection, absorption, and scattering, thereby lowering the irradiance available at the surface. Similar results have been reported in studies that identify cloud processes as one of the principal sources of irradiance variability and PV output fluctuation [11,13]. In the present Zambian context, the strong cloud–irradiance relationship provides the clearest explanation for the pronounced wet season suppression observed at the more humid northern and lake-proximate sites, and it shows that spatial differences in solar

resource performance are fundamentally linked to cloud persistence rather than to solar geometry alone.

(b) Relative humidity. Figure 9 shows that relative humidity also maintained a consistently negative relationship with irradiance across the sites.

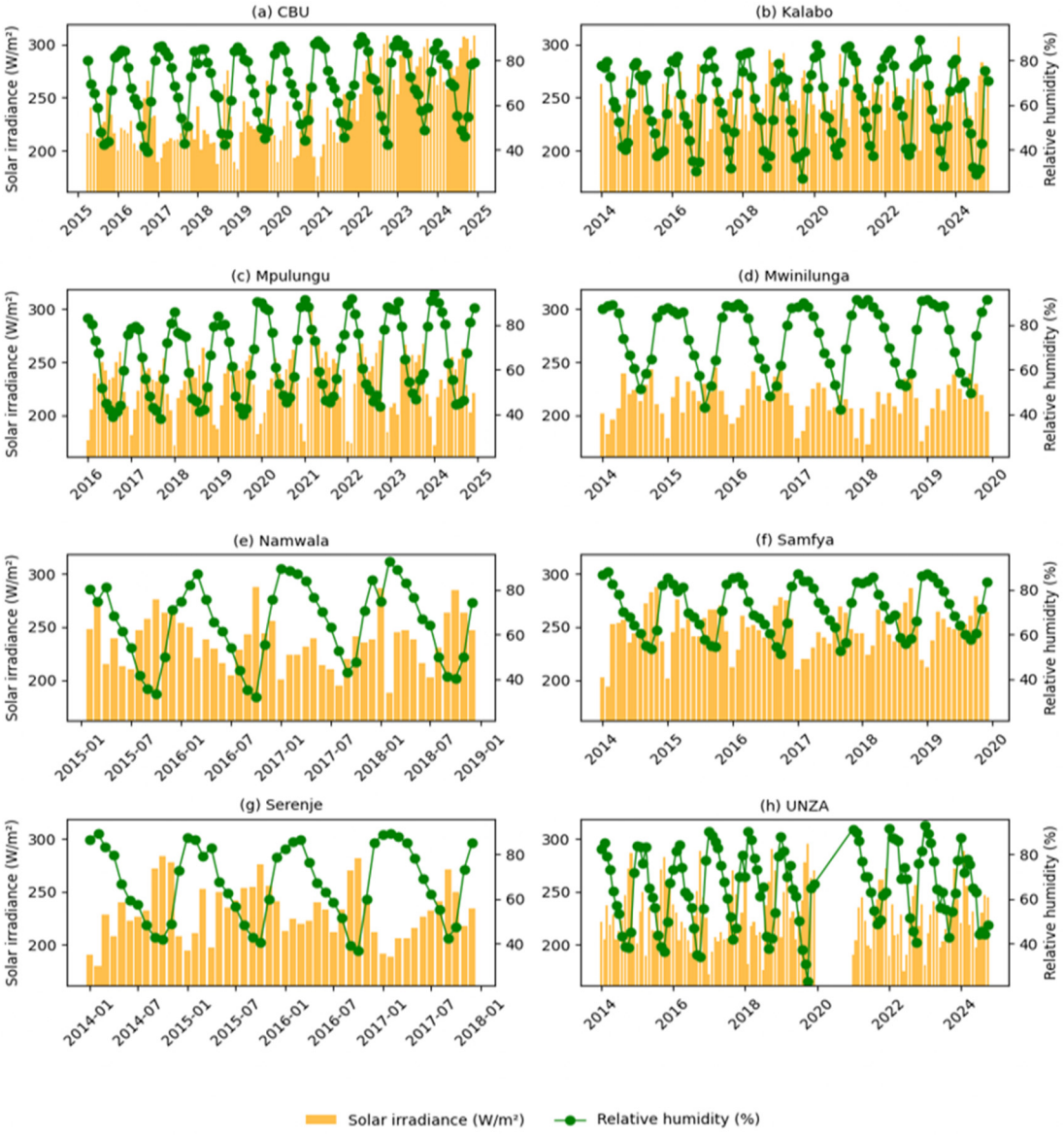


Figure 9. Relationship between relative humidity and global solar irradiance across the study sites.

The observed influence of relative humidity on solar irradiance variability in Figure 9 can be interpreted as both a direct and indirect indicator of reduced atmospheric transmissivity. High humidity commonly coincides with air masses rich in moisture, enhanced cloud formation, and greater scattering conditions, all of which reduce the amount of solar radiation reaching the surface. This interpretation aligns with [26], which identified humidity as an important environmental determinant of PV performance, and with [7], which showed that humidity-related atmospheric effects can reduce PV-relevant irradiance conditions. In this study, the negative humidity relationship clarifies why sites exposed to stronger wet-season moisture loading experience deeper irradiance minima and lower effective solar availability than the drier western and plateau sites.

(c) Precipitation: The relationship between solar irradiance and precipitation across the eight sites.

As illustrated in Figure 10, precipitation was negatively correlated with irradiance at all eight sites, indicating that rainfall months correspond to periods of reduced solar resource availability. This observation is in agreement with findings of previous studies that reported inverse relationships between rainfall and solar radiation, especially in tropical environments where wetter periods are accompanied by greater cloud cover, higher atmospheric moisture, and reduced transmissivity [27,28]. The stronger negative results observed at Mpulungu, Mwinilunga, and Samfya indicate that, in the wetter and more humid parts of Zambia, rainfall occurs within more persistent cloudy conditio2ns that continue to suppress solar irradiance beyond the timing of individual rainfall events. Precipitation is not an isolated solar irradiance variability driver. It is a visible manifestation of the broader cloud- and moisture-rich atmospheric regime associated with irradiance suppression.

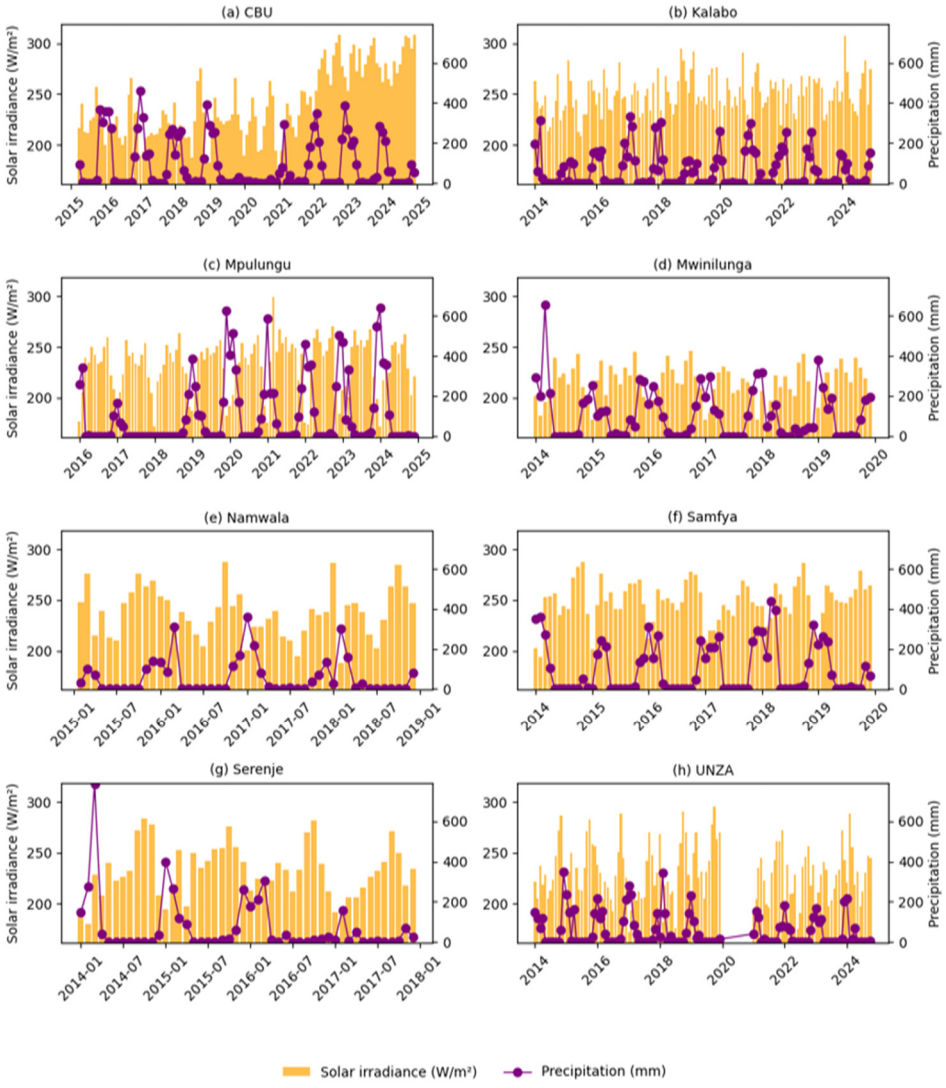


Figure 10. Relationship between monthly precipitation and global solar irradiance across the study sites.

(d) Air temperature. Figure 11 indicates a positive relationship between air temperature and irradiance across the eight sites.

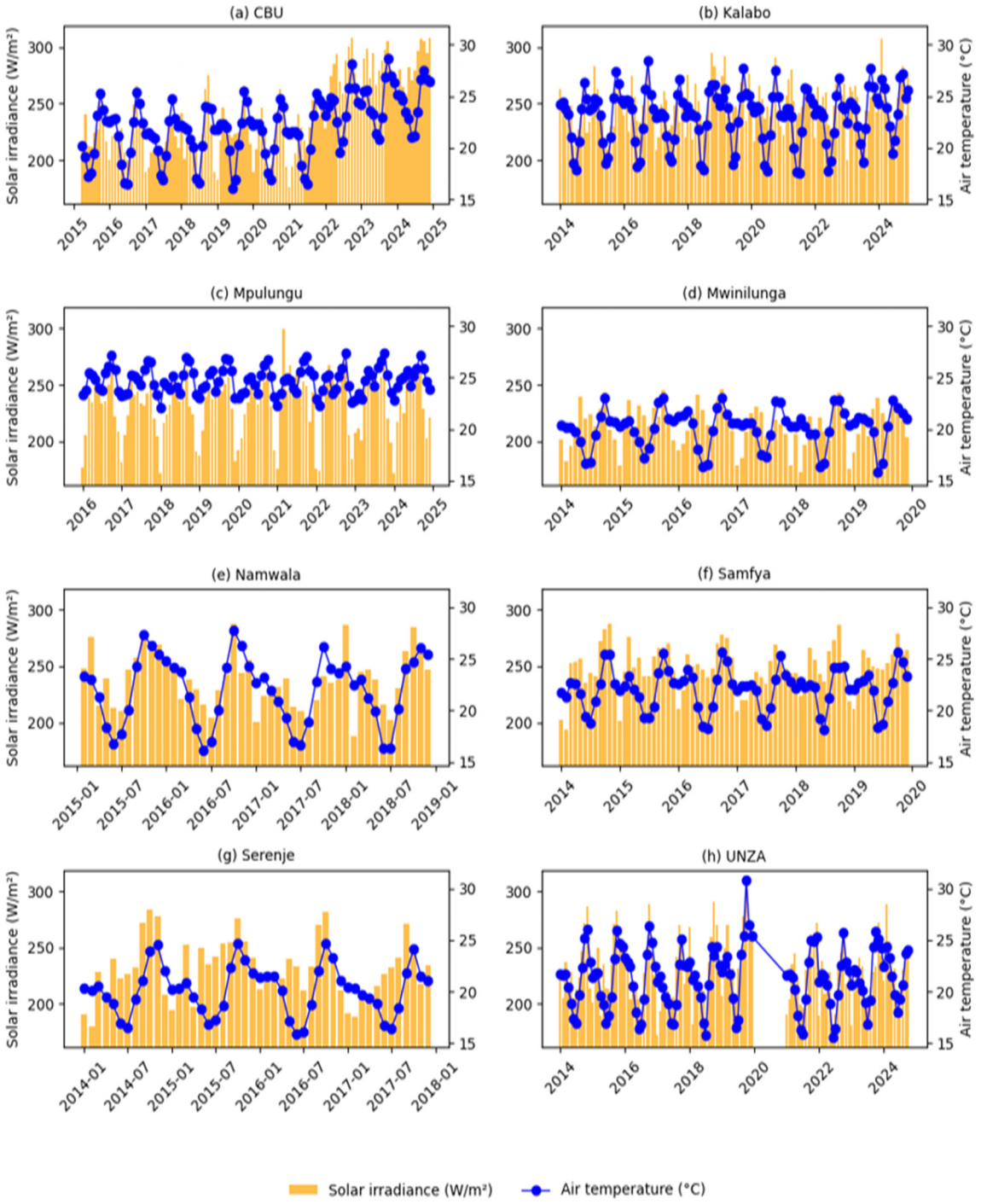


Figure 11. Relationship between air temperature and global solar irradiance across the study sites.

This observed positive correlation in Figure 11 reflects seasonal variation, with highest-irradiance periods coinciding with warmer conditions, especially during the dry and hot seasons preceding the rains. This means that temperature is not a driver of solar irradiance variability but can act as a climatic marker of high-solar-irradiance resource periods. This aligns well with the literature on PV performance which shows that irradiance and temperature often rise together seasonally, even though an elevated module temperature can reduce electrical efficiency at the modular level [12,14].

(e) Wind speed. Figure 12 shows that wind speed had the most spatially heterogeneous association with irradiance.

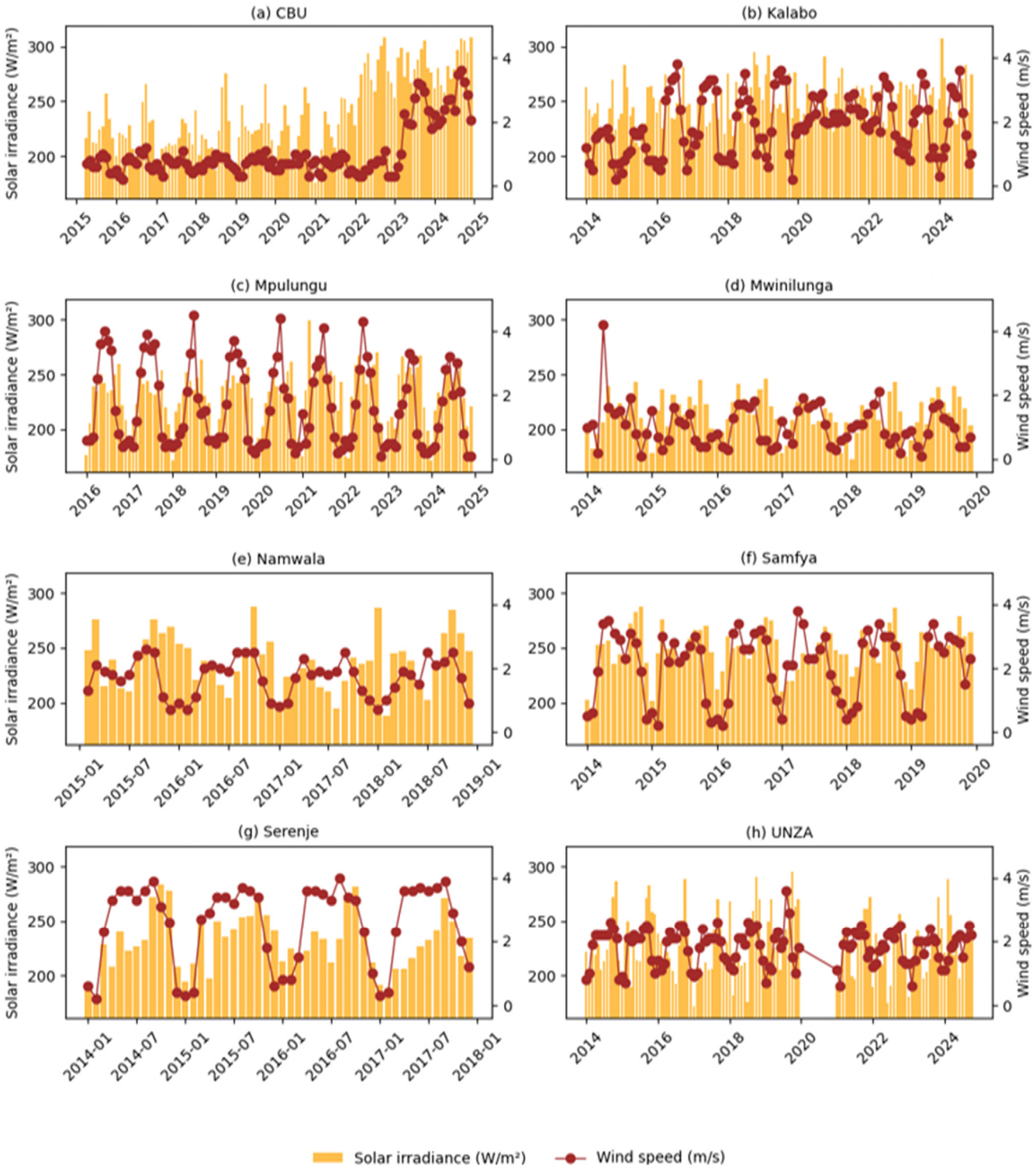


Figure 12. Relationship between wind speed and global solar irradiance across the study sites.

Moderate positive correlations were observed at Kitwe, Serenje, Mpulungu, and Samfya. However, UNZA (Lusaka), Namwala, and Mwinilunga all showed weak positive relationships and Kalabo showed a weak negative correlation. These patterns suggest that stronger winds coincide with dry-season conditions, which may favour boundary-layer mixing and promote improved atmospheric clarity. Conversely, weaker and negative relationships at other sites likely reflect local circulation effects, including floodplain moisture recycling at Kalabo, as well as mesoscale dynamics that decouple wind from cloud regimes.

Wind therefore operates as a secondary and site-dependent influence rather than as a systematic driver of irradiance variability.

The results show that irradiance variability in Zambia is controlled mainly by atmospheric transparency, especially cloud amount, relative humidity, and precipitation. Temperature and wind have more conditional effects. The findings further show that solar resource variability cannot be explained adequately by annual mean values alone, because local meteorological regimes regulate the seasonal and spatial transmission of solar radiation. This clarifies why northern and lake-influenced sites experience deeper low-solar-resource conditions than the drier western and plateau sites. The study therefore contributes new multi-site evidence from Zambia by linking meteorological drivers directly to spatial and seasonal irradiance variability across contrasting environments, rather than treating the country as a uniform solar resource zone.

3.7. Bivariate Analysis of Meteorological Drivers of Solar Irradiance Variability

To explore further the influence of atmospheric conditions on solar resource variability, a heat map was constructed to show site-specific bivariate correlations between monthly global solar irradiance and cloud amount, relative humidity, precipitation, air temperature, and wind speed across the eight study sites, as shown in Figure 13.

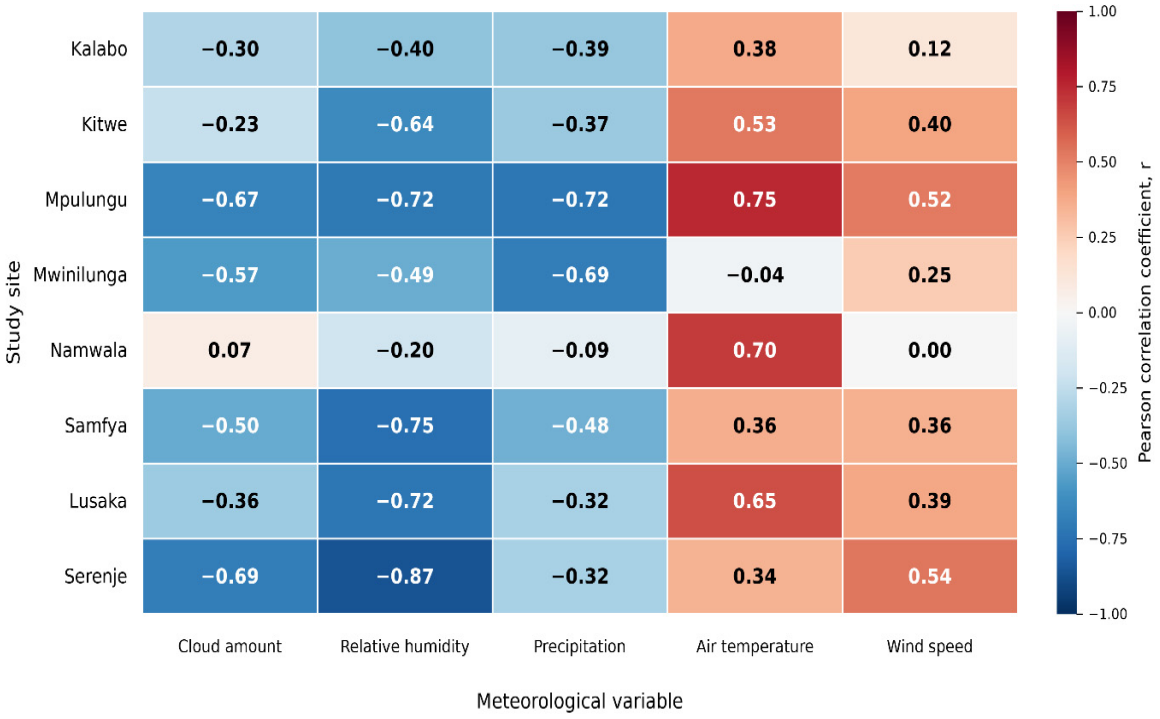


Figure 13. Heat map of site-specific associations.

The heatmap shows both the direction and magnitude of correlations across the sites. For example, at Mpulungu and Serenje, there is evidence of strong negative correlations with cloud amount and humidity. By contrast, positive associations with air temperature are most pronounced at Namwala and Lusaka. Wind speed also shows weaker but generally positive effects, with notable variability across sites.

In addition to the heat map, Pearson correlation coefficients are presented with 95% confidence intervals to indicate the precision of the estimated meteorological-irradiance associations. These graphs (in Figure 14) distinguish dominant drivers such as relative humidity, precipitation and cloud amount from weaker and more uncertain influences like wind speed.

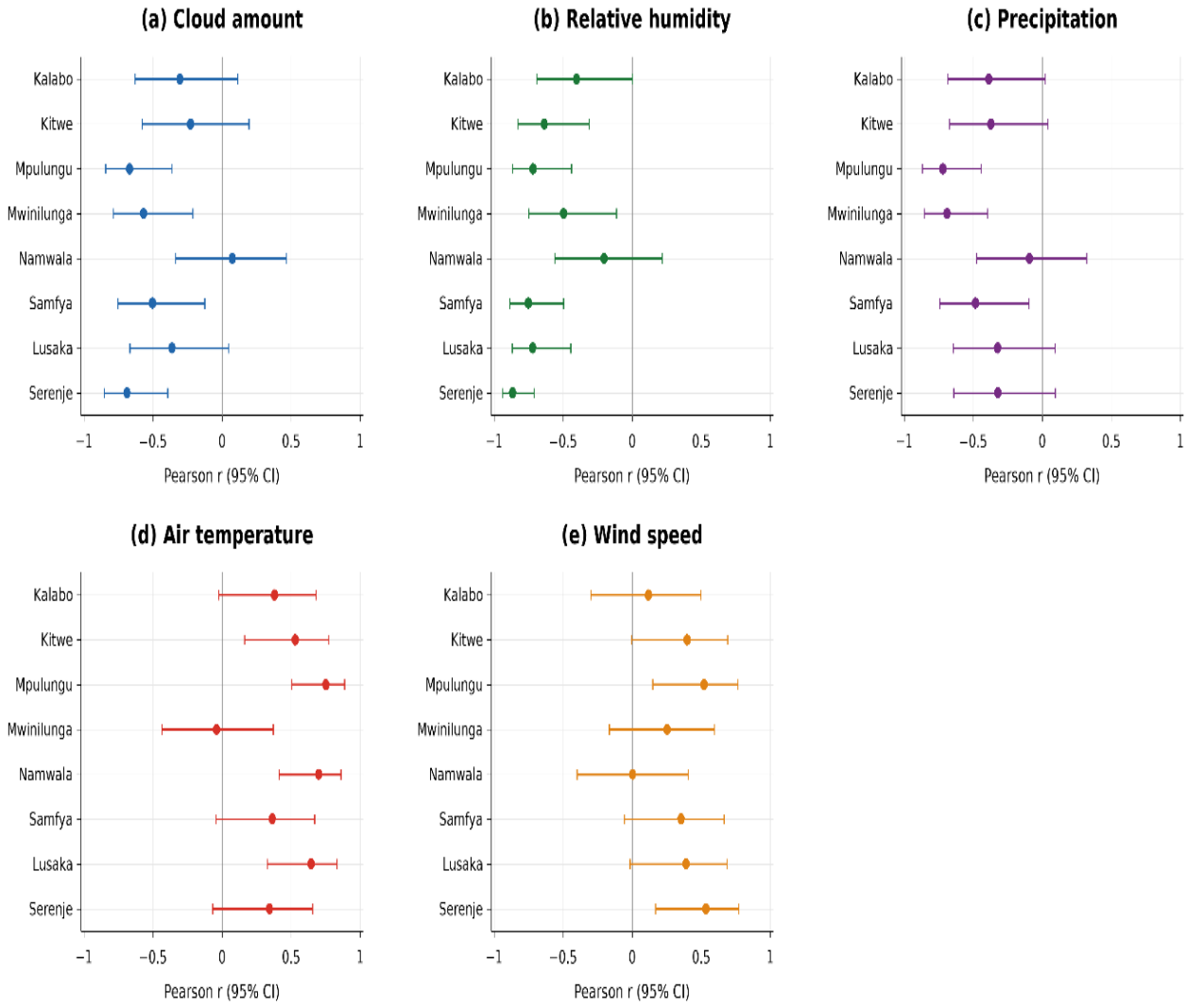


Figure 14. Pearson correlation coefficients with confidence intervals.

3.8. Solar Energy Applications

Table 5 presents the calculated days of autonomy (DoA) for PV battery bank sizing at each study site using site-specific daily and worst-month irradiance conditions. The results provide a quantitative assessment of the practical advantage of the proposed site-specific approach over the use of a uniform national worst-month design assumption. They show how local differences in the timing and severity of minimum solar resource conditions translate into different PV battery bank requirements.

The calculated days of autonomy (DoA) derived from site-specific daily and monthly average irradiance data shows that PV battery bank sizing requirements for stand-alone systems is sensitive to local solar resource behaviour. The differences in worst-month solar resource translates into differences of up to 1–2 days in DoA across the range of array-oversize factors (CA) considered. For a given daily load, such a change in DoA may correspond to a tens-of-percent variation in required battery capacity, with direct implications for system cost, reliability, and lifecycle performance.

These results indicate that adopting a single national 'worst-month' irradiance value would either oversize storage in some locations or undersize it in others, thereby compromising either economic efficiency or supply security. The site-specific days of autonomy values may point to the practical significance of improved, location-resolved solar resource accuracy for forecasting and planning PV systems in Zambia and similar environments.

Table 5. Calculated days of autonomy (DoA) for specific locations.

Location	DoA		
	CA 1.0	**CA 1.1**	**CA 1.25**
Kitwe	9.6	3.4	2.1
Kalabo	6.6	2.8	1.7
Mpulungu	5.2	2.8	1.5
Mwinilunga	4.7	2.4	1.5
Namwala	3.3	2.5	2.2
Samfya	6.1	3.8	2.2
Serenje	4.7	2.3	1.7
Lusaka	8.0	3.8	2.6

Furthermore, the observed associations between solar irradiance and wind speed, though weaker than those with cloud amount or humidity, suggest opportunities for hybridisation in regions where autonomy values are high. This may lower cost and reduce dependence on oversized battery banks, thereby improving system resilience.

In addition, sites adjacent to large water bodies, such as Samfya and Mpulungu, present unique challenges due to elevated humidity and cloud cover. Floating PV deployment in these locations may offer dual benefits: mitigating land-use competition while enhancing module cooling and reducing evaporation losses.

Additionally, the positive correlation between temperature and solar resource may suggest that module efficiency is vulnerable to heat stress, especially in Zambia where solar panels are often mounted directly onto iron sheets on many rooftops. Policy measures promoting raised or ventilated rooftop stands would enhance rooftop performance and durability. Further research into bifacial applications could unlock efficiency gains in semi-arid environments like Kalabo.

4. Conclusions

This study investigated the meteorological drivers of solar irradiance variability across eight sites in Zambia. It revealed clear seasonal and spatial contrasts in solar resource availability. Irradiance was generally higher and more stable at some western (Kalabo) and central sites, but lower and more strongly suppressed at northern (Mwinilunga) and lake-influenced locations (Mpulungu). The analysis further highlighted a regionally stratified worst-month pattern, with January emerging as the critical low-resource month at the wetter northern and lake-proximate sites, while June to July was more limited at the plateau, western, and southern sites. Sunshine duration also followed a clear seasonal pattern, increasing from the rainy season into the dry season, implying that atmospheric transparency, rather than day length alone, is a key driver of irradiance availability. The dominance of cloud amount, humidity, and precipitation as negative drivers highlights the spatially diverse nature of solar resource variability. This diversity is mirrored in the DoA results, which show that PV battery bank sizing, especially for stand-alone systems, must adapt to local solar conditions rather than rely on a uniform national benchmark.

Future research should incorporate longer and more spatially consistent observational records, aerosol-related variables, and ground-based, higher-resolution cloud and sunshine duration records. It should also quantify uncertainty in site-level irradiance estimates through confidence intervals and apply formal hypothesis tests to evaluate differences among stations, thereby strengthening inferential comparison and predictive modelling

beyond the scope of this study. By showing that Zambia's solar resource is spatially heterogeneous, seasonally stratified, and influenced by distinct meteorological drivers, this study provides an empirical foundation for more site-specific, climate-responsive, and reliable photovoltaic assessment and planning in the country and in the wider sub-Saharan region.

Author Contributions: Conceptualization, H.L. and R.R.; Methodology, H.L. and O.M.; Software, H.L.; Validation, R.R., R.O.M. and O.M.; Formal analysis, H.L.; Investigation, H.L.; Resources, H.L., R.R., R.O.M. and O.M.; Data curation, H.L.; Writing—original draft preparation, H.L., R.R., R.O.M. and O.M.; Writing—review and editing, H.L., R.R., R.O.M. and O.M.; Visualization, H.L.; Supervision, R.R., R.O.M. and O.M.; Project administration, R.R., R.O.M. and O.M.; Funding acquisition, H.L., R.R. and R.O.M. All authors have read and agreed to the published version of the manuscript.

Funding: This work was supported by the European Union's Horizon Europe Research and Innovation Programme under grant agreement no. 101118217 (RE-INTEGRATE project).

Data Availability Statement: The ground-based meteorological data used in this study were obtained from the SASSCAL weather-station network through the Department of Geographical Sciences, Environmental and Planning, University of Zambia. These data are not publicly available for redistribution by the authors; access is subject to permission from the data provider. Requests for access may be directed to the corresponding author, who can facilitate communication with the provider. The complementary NASA POWER data are publicly available through the NASA POWER platform. Sunshine-duration estimates were generated using Meteonorm, version 8.2.0, and their redistribution is subject to the applicable licence terms.

Acknowledgments: The authors gratefully acknowledge the Department of Geographical Sciences, Environmental and Planning, University of Zambia, for facilitating access to the SASSCAL dataset.

Conflicts of Interest: The authors declare no conflict of interest.

References

1. Bowa, K.C. Solar photovoltaic energy progress in Zambia. In Proceedings of the 2017 Southern African Universities Power Engineering Conference (SAUPEC), Stellenbosch, South Africa, 30 January–1 February 2017; pp. 471–476.
2. International Energy Agency. *World Energy Outlook 2022*; IEA: Paris, France, 2022. Available online: https://www.iea.org/reports/world-energy-outlook-2022 (accessed on 17 March 2026).
3. World Bank Group and ESMAP. *Solar Resource and PV Potential of Zambia: Solar Resource Atlas*; World Bank: Washington, DC, USA, 2019. Available online: https://documents1.worldbank.org/curated/en/139281556198757322/pdf/Solar-Resource-and-PV-Potential-of-Zambia-Solar-Resource-Atlas.pdf (accessed on 15 July 2026).
4. Imasiku, K. A solar photovoltaic performance and financial modeling solution for grid-connected homes in Zambia. *Int. J. Photoenergy* **2021**, *2021*, 8870109. [CrossRef]
5. Kapumpu, C.; Chisale, P.; Kwendakwema, N.; Luwaya, E. Predicting Global Solar Radiation on A Horizontal Surface: A Case Study For Zambia. *J. Nat. Appl. Sci.* **2020**, *4*, 33–41. [CrossRef]
6. Bloomfield, H.C.; Wainwright, C.M.; Mitchell, N. Characterizing the variability and meteorological drivers of wind power and solar power generation over Africa. *Meteorol. Appl.* **2022**, *29*, e2093. [CrossRef]
7. Sarmah, P.; Das, D.; Saikia, M.; Kumar, V.; Yadav, S.K.; Paramasivam, P.; Dhanasekaran, S. Comprehensive analysis of solar panel performance and correlations with meteorological parameters. *ACS Omega* **2023**, *8*, 47897–47904. [CrossRef] [PubMed]
8. Asian and Pacific Centre for Transfer of Technology. *Solar Energy Resource Assessment Handbook*; APCTT: Bangkok, Thailand, 2009.
9. Polo, J.; Martín-Pomares, L.; Sanfilippo, A. (Eds.) *Solar Resources Mapping: Fundamentals and Applications*; Springer: Cham, Switzerland, 2020. [CrossRef]
10. Barry, M.L.; Steyn, H.; Brent, A.C. Determining the most important factors for sustainable energy technology selection in Africa. *S. Afr. J. Ind. Eng.* **2009**, *20*, 33–55. [CrossRef]
11. Barry, T. *Infrastructure and Climate Change: Sustainable Infrastructure Series—A Global Leadership Forum Discussion Paper*; International Federation of Consulting Engineers (FIDIC): Geneva, Switzerland, 2023. Available online: https://fidic.org (accessed on 23 February 2026).
12. Hassan, A.A.; Atia, D.M.; El-Madany, H.T.; Eliwa, A.Y. Performance assessment of a 30.26 kW grid-connected photovoltaic plant in Egypt. *Clean Energy* **2024**, *8*, 120–133. [CrossRef]

13. Bamisile, O.; Acen, C.; Cai, D.; Huang, Q.; Staffell, I. The environmental factors affecting solar photovoltaic output. *Renew. Sustain. Energy Rev.* **2025**, *208*, 115073. [CrossRef]
14. Hasan, K.; Yousuf, S.B.; Tushar, M.S.H.K.; Das, B.K.; Das, P.; Islam, M.S. Effects of different environmental and operational factors on the PV performance: A comprehensive review. *Energy Sci. Eng.* **2022**, *10*, 656–675. [CrossRef]
15. Khatib, T.; Ibrahim, I.A.; Mohamed, A. A review on sizing methodologies of photovoltaic array and storage battery in a standalone photovoltaic system. *Energy Convers. Manag.* **2016**, *120*, 430–448. [CrossRef]
16. Palmer, D.; Koubli, E.; Cole, I.; Betts, T.; Gottschalg, R. Satellite or ground-based measurements for production of site-specific hourly irradiance data: Which is most accurate and where? *Sol. Energy* **2018**, *165*, 240–255. [CrossRef]
17. Markvart, T.; Fragaki, A. *PQS Solar Autonomy Calculation Method*; University Southampton and World Health Organization Performance, Quality and Safety Programme: Southampton, UK, 2011. Available online: https://extranet.who.int/prequal/key-resources/documents/solar-autonomy-calculation-method (accessed on 10 December 2025).
18. Vindel, J.M.; Sancho, J.M.; García, J.A. Temporal and spatial variability analysis of the solar radiation in a region affected by the intertropical convergence zone. *Meteorol. Appl.* **2020**, *27*, e1824. [CrossRef]
19. Ohajianya, A.C.; Ouserigha, E.C.; Ezihe, J.A.; Nwaneho, F.U.; Okereke, B.O.; Echewodo, C.M.; Ugbaja, C.M.; Shehu, M. Solar irradiance variability and its impact on PV-battery standalone system sizing and techno-economic performance across different climatic regions. *J. Sol. Energy Res.* **2026**, *11*, 3055–3077. [CrossRef]
20. Southern African Science Service Centre for Climate Change and Adaptive Land Management. SASSCAL WeatherNet [Data Set]. 2024. Available online: https://www.sasscalweathernet.org (accessed on 20 June 2026).
21. National Aeronautics and Space Administration. POWER: Prediction of Worldwide Energy Resources [Data Set]. 2024. Available online: https://power.larc.nasa.gov (accessed on 19 July 2026).
22. Remund, J.; Müller, S.; Schilter, C.; Rihm, B. *Meteonorm Handbook Part I: Software, Version 8.0*; Meteotest AG: Bern, Switzerland, 2020.
23. Australian Government Bureau of Meteorology. Solar and Terrestrial Radiation—Glossary. 2020. Available online: http://www.bom.gov.au/climate/austmaps/solar-radiation-glossary.shtml (accessed on 3 June 2026).
24. Roderick, M.L. *Methods for Calculating Solar Position and Day Length Including Computer Programs and Subroutines*; Report 137; Department Primary Industries and Regional Development: Perth, WA, Australia, 1992. Available online: https://library.dpird.wa.gov.au/rmtr/123 (accessed on 23 June 2026).
25. Mwanza, M.; Chachak, J.; Çetin, N.S.; Ülgen, K. Assessment of solar energy source distribution and potential in Zambia. *Period. Eng. Nat. Sci.* **2017**, *5*, 103–116. [CrossRef]
26. Hasan, D.S.; Farhan, M.S.; Alrikabi, H.T.S. Impact of cloud, rain, humidity, and wind velocity on PV panel performance. *Wasit J. Eng. Sci.* **2022**, *10*, 34–43. [CrossRef]
27. Dramé, M.S.; N'Diaye, P.M.; Niang, S.A.A.; Diallo, I.; Sarr, A.; Gueye, A.; Niang, D.N. On the characterization of cloud occurrence and its impact on solar radiation in Mbour, Senegal. *J. Atmos. Sol.-Terr. Phys.* **2024**, *261*, 106284. [CrossRef]
28. Al-Waeli, A.H.A.; Kazem, H.A.; Chaichan, M.T.; Sopian, K. *Photovoltaic/Thermal (PV/T) Systems: Principles and Applications*; Springer: Cham, Switzerland, 2022.

Disclaimer/Publisher's Note: The statements, opinions and data contained in all publications are solely those of the individual author(s) and contributor(s) and not of MDPI and/or the editor(s). MDPI and/or the editor(s) disclaim responsibility for any injury to people or property resulting from any ideas, methods, instructions or products referred to in the content.